Journal of Petroleum
Science and Technology

An Experimental Investigation into the Effects of High Viscosity and Foamy Oil Rheology on a Centrifugal Pump Performance

Hiep Phan[1]*, Tan Nguyen[1], Eissa Al-Safran[2], Olav-Magnar Nes[3], and Arild Saasen[3]

[1]Department of Petroleum Engineering, New Mexico Institute of Mining and Technology, New Mexico, United States
[2]Kuwait University, Kuwait
[3]Det Norske Oljeselskap ASA, Norway

ABSTRACT

This paper presents the effect of high viscosity oil and two-phase foamy-oil flow on the performance of a single stage centrifugal pump. As a part of this, the applicability of a pipe viscometer to determine the foamy oil viscosity is investigated. Unlike previous studies, a sealed fluid tank is used in a closed flow loop to allow conditioning the two-phase mixture to create foamy-oil. Furthermore, the sealed tank enables the accurate determination of the gas void fraction (GVF) of the foamy-oil under steady state conditions. The results show that up to a GVF of 38%, the foamy-oil improves head performance in comparison with the single-phase pump performance. In addition, the viscosity of foamy oil is found to be similar to the single-phase oil due to the Newtonian behavior of foamy oil. New correction factors have been developed to predict the performance of a single-stage centrifugal pump handling foamy oil.

Keywords: Centrifugal Pump Performance, Two-phase Foamy Oil, Electrical Submersible Pump Performance, Foamy Oil Viscosity

INTRODUCTION

Artificial lift methods are often used in wells with insufficient reservoir pressure to achieve desirable oil production. In such cases, ESP is commonly applied, especially in offshore wells, due to its flexibility, operational temperature range, a relatively small surface control facility, and a high production rate. The electrical submersible pump is a multi-stage centrifugal pump, inheriting the shortcomings of a single-stage centrifugal pump. Many factors; such as, viscosity, gas or solid presence, and rotational speed could greatly deteriorate the pump performance. Furthermore, it is common to have free gas in oil wells. However, the two-phase oil-gas effect on centrifugal pump performance is not fully understood. Most of the research on two-phase centrifugal pump and ESP performance has been performed with water and air [1-5]. A few studies have investigated the viscous effects on two-phase liquid-gas pump performance, but none of them has studied the effects of high viscosity, high gas volume fraction (GVF), and foamy-oil effects on a centrifugal pump performance [5-6].

Foamy oils are characterized as heavy (or high

***Corresponding author**
Hiep Phan
Email: hphan@nmt.edu
Tel: +71 44176432
Fax: +57 58355210

Article history
Received: October 08, 2015
Received in revised form: March 16, 2016
Accepted: April 04, 2016
Available online: February 20, 2017

viscosity) oils with the stable presence of tiny gas bubbles. The foaminess often persists in open vessels for several hours [7], which would suggest that the interaction between these small bubbles be much less energetic compared to a low viscosity mixture such as a water-air mixture. In water-air mixtures, the gas bubbles would quickly coalesce to form bigger bubbles, which would eventually separate from the liquid phase. For solution-gas-drive heavy oil wells, it is often observed that foamy-oil reservoirs exhibit an anomalously high production rate and a primary recovery factor, exceeding the prediction using Darcy's Law [8]. To explain such an unusual outcome, various theories have been proposed; besides, some of theories have been suggesting that the effect be caused by a viscosity difference between the foamy-oil and the single-phase oil. Most recently, Alshmakhy and Maini have used three different types of viscometers (i.e. electromagnetic viscometers, capillary tubes, and sand-packed slimtubes), and concluded that foamy-oil viscosity has been similar to that of a live oil up to a GVF of 40% [9].

The electrical submersible pump can readily generate the foamy-oil as documented by Solano [10]. He noted that the micro-foam existence has also persisted in atmospheric conditions for several hours; moreover, the foamy sample has exhibited a color change compared to the single-phase oil. The occurrence of foamy-oil can be explained based on previous studies on two-phase water-air pump performance. In visualization studies of two-phase flow, upstream stages have been shown to act as "flow conditioners" or "bubble breakers" for downstream stages [11-12]. To improve the understanding of two-phase viscous oil and gas effects on a single-stage centrifugal pump performance, and to extend the ESP downstream stages performance, the objective of this paper is to gather pump performance experimental data under single-phase viscous flow and two-phase highly viscous foamy oil at different GVF's. At the same time, the study intends to investigate the rheology of foamy oil using the pipe viscometer.

EXPERIMENTAL PROCEDURES

Experimental Facility

A schematic of the facility is presented in Figure 1. The liquid is stored in the reservoir tank with a capacity of 170 liters, which is elevated above the AC centrifugal booster pump to avoid cavitation. The reservoir tank can either be exposed to the atmosphere or be pressurized with a sealed lid on top. The fluid temperature is controlled using a manually operated heater installed at the bottom of the tank. To ensure the uniform fluid temperature in the tank, a variable speed propeller has been used to stir the fluid when the tank is exposed to the atmosphere. When the tank is pressurized, a heavy metal lid with a rubber gasket is placed on the top of the tank. The lid is equipped with a small port for the placement of the Omegaette RTD temperature and the Rosemount 2051 pressure sensors.

The AC booster pump is placed underneath the reservoir tank and it only runs at 3600 rpm. The pump is then connected to the Endress+Hauser Promass 8°F Coriolis mass flowmeter, set up to show the volumetric flow rate in gallon per minute (gpm) and the temperature of the liquid or mixture in degrees Fahrenheit. Right after the flow meter, there is a gas injection port, connected to the nitrogen, supplying set-up of the facility. After the gas injection port, the liquid flows to the single-stage centrifugal pump, which is controlled by a variable frequency drive (VFD). The pressure generated by the pump is measured using a Rosemount 2051 differential pressure transmitter. The pipe viscometer installed downstream from the pump is used to monitor the rheology of the fluid exiting the centrifugal pump under the flowing condition. The pipe viscometer is a pipe section with two fitted ports, which are connected to another Rosemount 2051 differential pressure transmitter. A choke valve is placed after this setup to control the flow rate of the system. After the choke valve, the fluid stream returns to the tank.

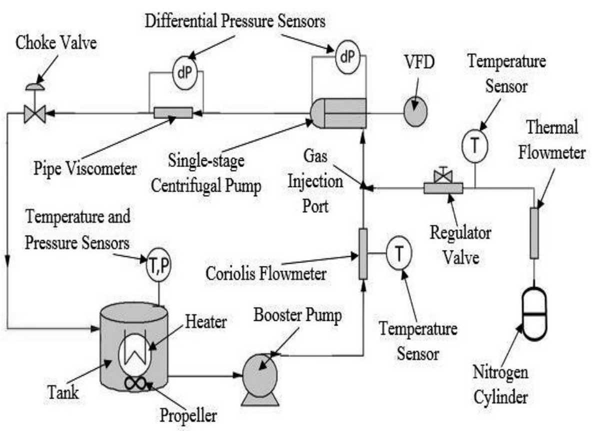

Figure 1: A schematic of the pump facility.

The gas which is needed for the study is supplied by nitrogen cylinders. The flow rate of the gas is measured by the Endress+Hauser t-mass 65F thermal mass flow meter. To control the flow rate of nitrogen, an analog gas regulator valve is employed. The temperature of the gas is monitored and recorded by the Omegaette RTD temperature sensor.

Test Fluids

For this work, the Conoco R&O Multipurpose 220, which is a Newtonian fluid, has been used. This reduces effects from variations due to the fluid rheology during testing. A viscosity-temperature curve produced by the Anton Paar MCR 302 rotational viscometer is shown in Figure 2. As expected, the viscosity of the fluid dropped non-linearly as the temperature increased from 21 to 66°C. In the lower temperature range, the reduction in viscosity has been much more significant. The reduction in viscosity illustrates that at lower temperature testing, extra effort would be needed to maintain the temperature constant to reduce fluctuations in viscosity. The density of the fluid was measured at the planned testing temperatures (from 43 to 49°C) using the mud balance, and was found to be constant at 865 kg/m^3.

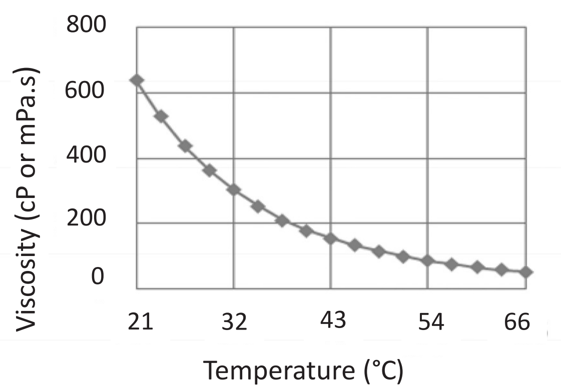

Figure 2: Oil viscosity-temperature curve; the nitrogen cylinder was pressurized to about 13.8 MPa.

Pipe Viscometer Rheology Measurements

Commonly used for research purpose and in-line viscosity measurements the pipe viscometer (Figure 3) can characterize the fluid under flowing conditions. A standard pipe viscometer system has a flow rate and pressure loss measuring instrumentations.

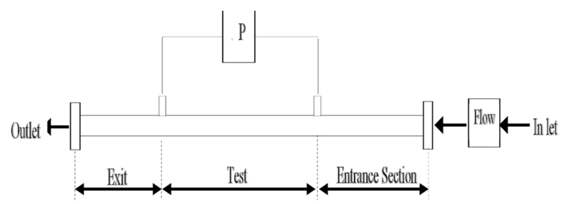

Figure 3: Pipe viscometer system.

The shear stress at the pipe wall can be calculated by using a given frictional pressure drop, the length of the pipe viscometer, and the radius of the pipe:

$$\tau_w = \frac{R}{2}\left(-\frac{\Delta P}{\Delta L}\right) \quad (1)$$

On the other hand, the shear rate at pipe wall can be calculated with the mean velocity (obtained from the flow meter) and the pipe diameter [13]:

$$\dot{\gamma}_w = \left(\frac{3N+1}{4N}\right)\frac{8U}{D} \quad (2)$$

where, N is the generalized flow behavior index, which can be determined as follows:

$$N = \frac{d\left(\ln \tau_w\right)}{d\left(\ln \frac{8U}{D}\right)} \quad (3)$$

The apparent viscosity of the fluid is then calculated based on the shear stress vs. the shear rate curve. In this facility, the length of the viscometer pipe section is 0.984 m and the internal diameter of the pipe is 0.0213 m.

Single-phase Oil Test

In all the tests, three temperatures (viscosities) were chosen: 43°C (155 cP), 46°C (134 cP), and 49°C (115 cP). To ensure the temperature uniformity during a test run, a propeller was used to mix the fluid inside the tank. The propeller was driven by a variable speed motor. At a high speed, the risk of creating a mixing vortex, which might lead to pump cavitation, was high. A trial run at 49°C at the maximum pump speed determined that mixing vortices would not occur below 75% of the maximum propeller speed. To confirm the absence of entrained gas, a sample of oil was taken for visual check. Extra precaution was also taken that the propeller motor was often operated at a half speed. Each viscosity test was run at three different centrifugal pump rotational speeds, in other words 3600, 3300, and 3000 rpm. For each viscosity and rotational speed combination, the pump performance test was repeated three times.

Two-phase Foamy oil Test

A two-phase foamy-oil test presented the largest challenge in this study. Most of the papers studying the effects of two-phase fluids on a centrifugal pump or an ESP have used air and water. In these studies, gas was injected constantly into the liquid phase. A conventional separator is sufficient to separate the gas out of the liquid before the liquid returns back into the tank. The ratio between the volumetric rate of gas injection and the volumetric rate of the liquid in in-situ condition would be the gas-oil-ratio (GOR):

$$GOR = \frac{Q_g}{Q_o} = \frac{V_g}{V_o} \quad (4)$$

However, this approach was not suitable for conducting our tests because of two reasons: (1) commercial separators are not able to separate gas out of high viscous fluid, and hence the GVF is undetermined; (2) continuously injecting gas into the liquid phase leads to difficulty in attaining the foamy state because it would require conditioning of the oil-gas mixture by a single-stage centrifugal pump to have a foamy mixture.

To solve this issue, the liquid tank was modified into a pressurized tank. A metal lid with a rubber gasket was put on top of the tank to trap any escaped gas, which would increase the pressure inside the tank. The total amount of gas injected was measured by the flow meter and the amount of free gas escaped from the oil during injection was monitored by the pressure increase inside the liquid tank. The volume of the remaining gas inside the oil could then be calculated based on the ideal gas law. With the known oil volume, the GOR of the mixture was calculated as the ratio between the remaining gas volume in the oil and the volume of the oil, as defined in Equation 4.

In order to check if the liquid tank held the testing pressures, two trial runs would be conducted to find the maximum holding pressure as illustrated in Figure 4. The first trial run was carried out for 110 minutes at 193 kPa. The second trial run was tested for almost four hours at 345 kPa. The results from the two runs revealed that the tank could hold pressure well for pressures up to 345 kPa. In this study, all the tests were carried out at pressures in the system of less than 276 kPa. Therefore, the seal should be able to maintain the pressure during the actual experiments.

For the data analysis, not only did the gas pressure inside the tank have to be determined, but the temperature of the gas also needed to be measured. A temperature probe was installed on top of the tank to measure the gas temperature inside the tank. This temperature, together with the gas pressure, was utilized to calculate the amount of free gas inside the tank.

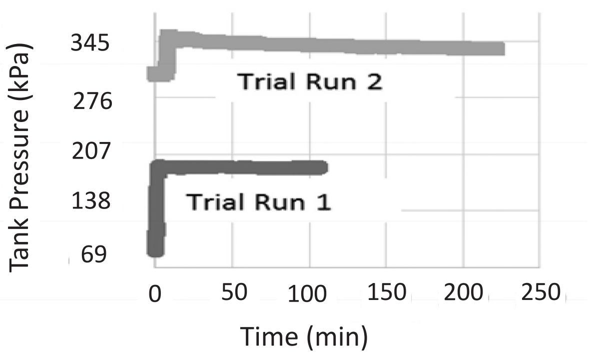

Figure 4: Transient Tank pressure; trial Run 1 confirms that the tank can hold the applied pressure for the experiment (193 kPa); trial Run 2 identifies the maximum pressure the tank can hold (about 345 kPa).

For the two-phase pump performance test, the selected temperatures were 43, 46, and 49°C. At each temperature, the same three rotational speeds were used as in the single-phase, viscous test: 3600, 3300, and 3000 rpm. Finally, there were four GOR's tested during each test. The GOR was determined by the duration of gas injection, namely 1, 3, 6, and 9 minutes at a constant gas injection rate. For two-phase tests, a matrix of three temperatures, three rotational speeds, and four GOR's were planned. From the GOR, The GVF λ_g was then calculated as follows:

$$\lambda_g = \frac{GOR}{1+GOR} \tag{5}$$

Equation 5 can be used only under homogenous foamy-oil flow. This foamy-oil is treated as a homogeneous two-phase mixture. Therefore, under flowing condition, it is assumed that there is no slip between the tiny bubbles and the liquid phase. It was then found out that 150°F was the temperature needed to remove entrained gas and possible solution gas. Therefore, after each test, the fluid was heated up to at least 65°C. Then, it was allowed to cool down to the set temperature for another test run. Optimally, at each temperature and speed combination, each injection time could be built upon the previous one.

RESULTS AND DISCUSSIONS

Transient Behavior of the Testing Loop under a Two-phase Oil-gas Flow

Figure 5 shows how the Coriolis flowmeter, the pump, and the pipe viscometer behaved in one of the two-phase test runs. A typical two-phase test can be divided into four different stages:

Stage 1: as the gas is injected into the loop, the pump does not develop any pressure (i.e. under gas-lock condition). Trevisan and Prado (2010) characterized this condition in an intermittent gas pattern, under which the large bubbles are not broken up. At the same time, the liquid flow rate is greatly fluctuating. This is because the gas injection port, which is installed downstream of the liquid flowmeter, will exert a backpressure restricting the fluid flow.

Stage 2: when the gas injection is stopped and the liquid is kept circulating, the bubble size becomes smaller. As a result, the pump performance gradually recovers back to the steady state performance. During this initial period, the liquid flow rate drops significantly right after the gas shut-off. After a short phase of conditioning the fluid, the liquid flow rate rises and approaches a steady state flow rate. This behavior is because the oil-gas mixture re-circulates back into the loop. The initial large gas bubble size interferes with the flow of the mixture inside the Coriolis flowmeter.

Stage 3: as soon as the pump returns back to a steady state performance, the liquid flow rate and the pump reach a steady state indicating that the micro-sized bubbles have insignificant effects. During the recovery period after the gas injection shut-off and before reaching steady foamy flow, the pump intake pressure stays relatively constant. A 69-kPa increment in intake pressure right after steady state suggests that the booster pump should also reach a steady, higher performance state.

Stage 4: The different behaviors of the liquid rate and the intake pressure are obtained by adjusting the choke valve after the pipe viscometer. This step helps map the two-phase performance of the pump.

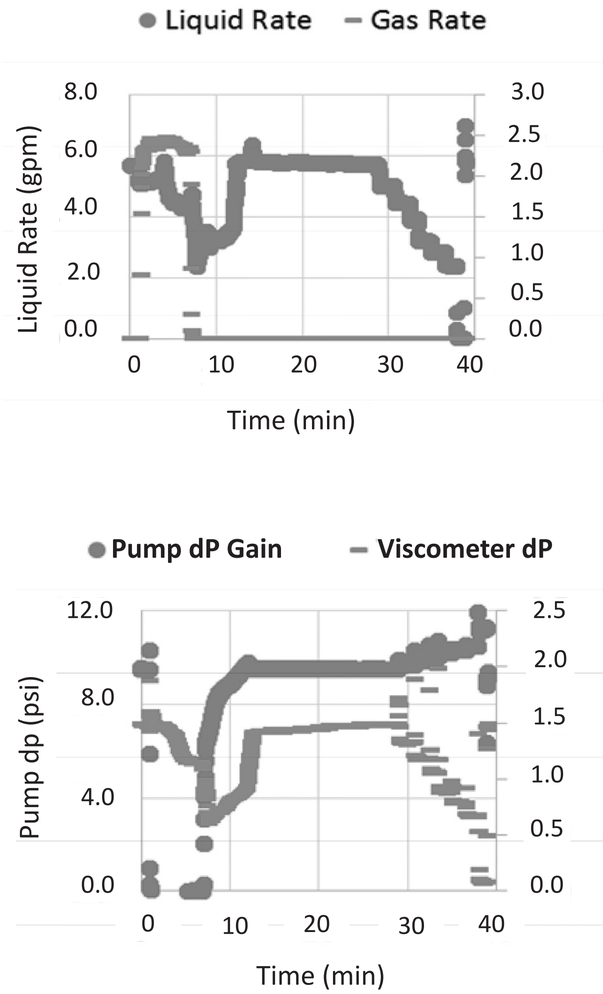

Figure 5: Transient behavior of the flowmeter, the pump, and the viscometer in one test run; Stage 1: gas injection, Stage 2: bubble breaking, Stage 3: homogeneous flow, and Stage 4: pump test.

Oil samples were collected before Stage 1 and after Stage 3 for visual demonstration (Figure 6). The original oil was translucent with an amber color. On the other hand, the foamy-oil mixture was cloudy and the color changed into yellow. The color change was due to tiny bubbles, which refracted light, not visible on the pictures. If the foamy oil were exposed to open air, its appearance would remain unchanged for hours, days, or even weeks depending on the ambient temperature.

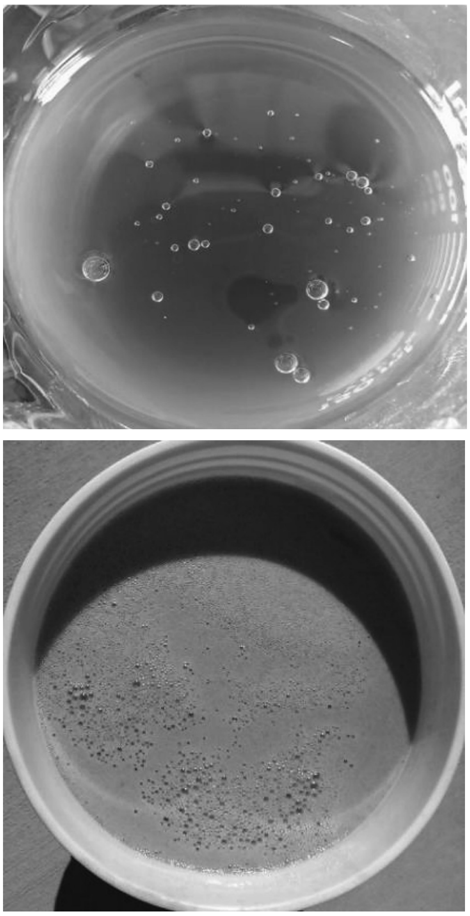

Figure 6: Single-Phase Oil (top) and Foamy-Oil (bottom)

Pipe Viscometer Measurements Analysis

Using Equations 1 to 3, the shear stress and shear rate under single-phase flow were calculated based on the pressure drop across the pipe viscometer and the flow rate of the oil at all three different rotational speeds (3600, 3300, and 3000 rpm). A linear trend line which was going through the origin was used to fit the analyzed data, and the slope of the line was the viscosity of the fluid; this trend line represented a Newtonian fluid. Table 1 shows the summary of the measured viscosities by the rotational viscometer and the calculated viscosities by the pipe viscometer under a single-phase flow. With the maximum error of 5.9%, there is strong agreement between the two viscometers. Thus, the pipe viscometers can be used with confidence to calculate the viscosity of the foamy oils. The fact that the calculation did not consider the pipe roughness might explain the higher error at higher viscosities.

Table 1: Rotational viscometer vs. pipe viscometer results under a single-phase flow.

Rotational Viscometer Measured Viscosities (cP)	Pipe Viscometer Calculated Viscosities (cP)	Error from the Measured (%)
155	146	5.9%
134	129	3.9%
115	114	1.4%

Similar calculations of pipe viscometer data were then performed under a two-phase foamy-oil flow. Figure 7 shows shear stress as a function of shear rate under a single-phase and foamy-oil flow of different viscosities at three different rotational speeds. The slope of the linear trend line is the fluid viscosity in centipoise. With up to a GVF of about 37.8% and several cool-heat cycles of the mixtures, the foamy-oils have similar viscosity as single-phase oil. This is similar to the findings by Alshmakhy and Maini [9]. Furthermore, foamy oils behave like a Newtonian fluid. Higher GVF data would be needed to find the critical GVF value, where the foamy oil rheology would deviate from the single-phase oil.

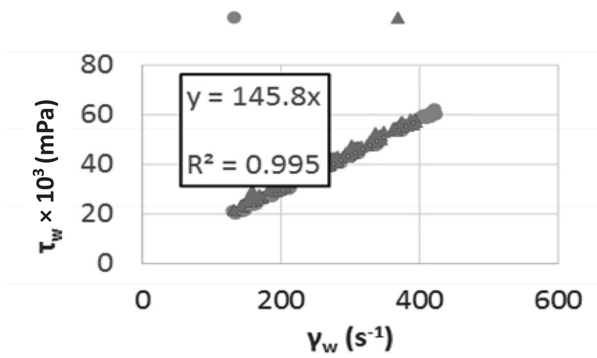

Figure 7: Shear stress vs. shear rate of 155 cP oil from 3000 to 3600 rpm for single-phase oil and foamy oils with a GVF of 11.4-37.8%.

Single-phase Oil vs. Two-phase Foamy Oils at 155 cP

To compare the single-phase and the two-phase foamy oil pump performance, the pump pressure increment was expressed as a function of a liquid-only flow rate. Under a foamy flow, the mixture flow rate was measured by the Coriolis mass flowmeter. This is because the foamy mixture can be treated as an incompressible homogeneous mixture, in which density only depends on the temperature of the mixture. With the measured mass flow rate and density, the flowmeter can calculate and display the volumetric flow rate of the foamy mixture. The liquid flow rate was then calculated as follows:

$$Q_l = Q_m \left(1 - \lambda_g\right) \tag{6}$$

Figure 8 presents the relationship between pump-developed pressure and the liquid flow rate under a single-phase and foamy oil flow at 155 cP and 3600 rpm. Single-phase oil is expressed as having a GVF of 0%. The solid curve of single-phase oil pump performance represents the average pump performance of the three test runs. At the same flow rate, the pump pressure under a two-phase foamy-oil, up to a GVF of 30%, are similar to that of the single-phase oil. This is atypical since given the same viscosity (as shown previously in the pipe viscometer data analysis), a centrifugal pump would give the same head performance regardless of the density of the fluid; as the fluid density decreases, the pump generates less ΔP to produce the same head (Equation 7). On the other hand, under a foamy-oil flow, there has been an additional pressure gain to compensate for the pressure loss due to the reduction in density. This pressure gain can be explained by less energy losses of foamy oil within the pump in comparison to that of the single-phase oil.

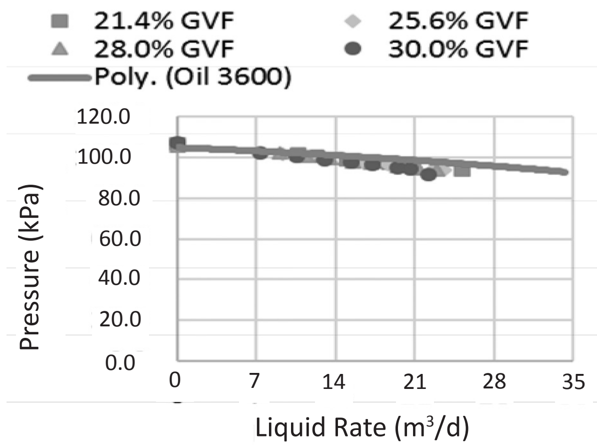

Figure 8: Single-phase oil vs. two-phase foamy oil pump performance at 155 cP and 3600 rpm.

The relationship between pump developed pressure and pump head is given by:

$$H = \frac{\Delta P}{0.052 \times \rho} \tag{7}$$

In the foamy oil case, the density of the mixture was calculated as follows:

$$\rho_m = \rho_{oil}\left(1 - \lambda_g\right) + \rho_{gas}\lambda_g \tag{8}$$

Figure 9 shows the pump head performance as a function of liquid flow rate under a single-phase oil (having a viscosity of 155 cP) and two-phase foamy oil flow at 3600 rpm with ASME (American Society of Mechanical Engineers) 95% uncertainty analysis of the head; a further explanation of the approach is presented in the Appendix. Since the pump pressure is similar between the single-phase oil and foamy oil (Figure 8), a higher-GVF, lower-density foamy mixture has a higher pump head performance. Despite having a similar viscosity as the single-phase oil and the appearance of a homogeneous mixture, it would not behave like a lower-density, single-phase oil. This behavior of foamy oil correlated well with the higher primary production under solution-gas-drive of the heavy-foamy-oil reservoir. Furthermore, the 95% confidence interval of the head shows highly precise measurement of each reading, less than 0.5% deviation from the mean.

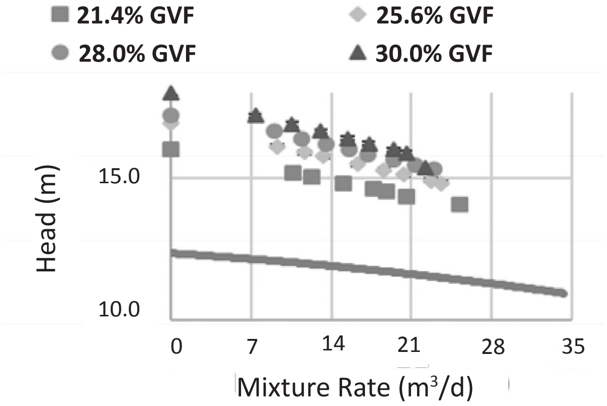

Figure 9: Single-phase oil vs. two-phase foamy oil head performance at 155 cP and 3600 rpm.

Homogeneous Model

Foamy oil appearance suggests its homogeneous nature. Thus, the experimental data was compared to the prediction of the homogeneous model (Hom.). Figure 10 shows that the homogeneous model under-predicts the pump pressure performance under a foamy flow up to 30% difference. Furthermore, the homogeneous model predicts that the higher the GVF is, the lower the pump pressure would become. This is because the homogeneous model assumes that the head performance will remain constant under a two-phase flow, while the two-phase pressure performance degrades due to the decrease in density. As a result, the homogeneous model is incapable of predicting the behavior of heavy-foamy oils.

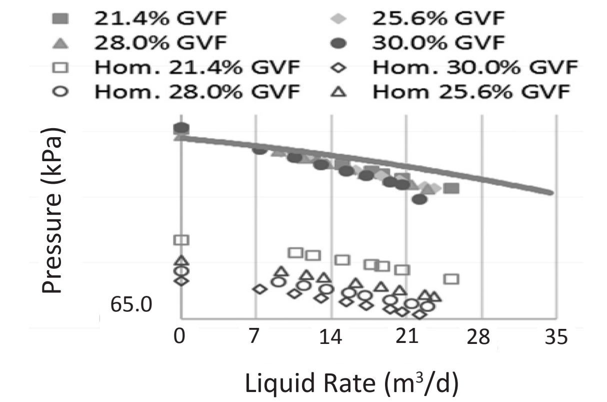

Figure 10: Oil pressure performance: experimental data vs. homogenous model at 155 cP and 3600 rpm.

Prediction Model

Based on the effect of foamy oil on the pump pressure and the head performance outlined in the single-phase oil vs. two-phase foamy-oils section, correction factors for head and capacity have been proposed:

$$C_{H_{foamy-oil}} = \left(\frac{\rho_{oil}}{\rho_{oil}\left(1-\lambda_g\right)+\rho_{gas}\lambda_g} \right) \tag{9}$$

$$C_{Q_{foamy-oil}} = \left(1-\lambda_g\right) \tag{10}$$

The single-phase oil head-capacity pump performance curve has measured at the facility and used as the base line. As seen in Figure 11, the correction head and capacity factors (in Equations 9 and 10) are then used to predict the performance of 155 cP foamy oils at four different GVF's: 16.4, 25.0, 34.2, and 37.8%. The difference between the modified model and experimental data is less than 3%. If only water head-capacity pump performance curve is available, other models which are predicting pump performance, such as the Hydraulic Institute chart, will be used to get the single-phase viscous pump performance curve first before applying the foamy correction factors in Equations 9 and 10.

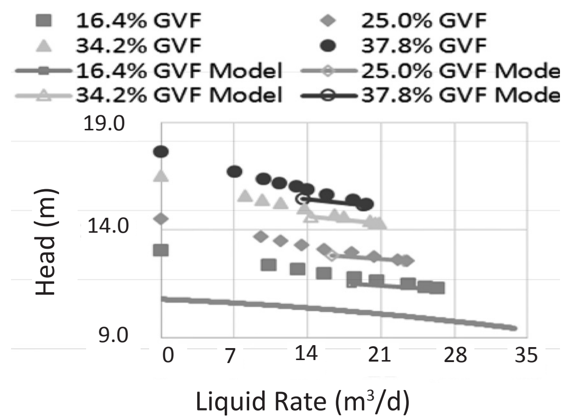

Figure 11: Head performance comparison: foamy correction model vs. experimental data.

APPENDIX

An experimental uncertainty assessment deals with analyzing the uncertainty in a measurement and determines how large an error might be in the result. During measurement in an experiment, the results will be affected by errors due to instrumentation, methodology, and other cofounding effects. The uncertainty analysis considered in this study is accepted by the American Society of Mechanical Engineering (ASME). An error consists of two main components: systematic error (bias) and random error (precision). Human error is assumed to be absent due to good engineering practice.

Systematic errors can come from various sources, but in this paper, only the instrumental errors as the major source are considered. Each instrument has its own elemental systematic uncertainty, bi. The combined effect of different instruments, Br¬, can be calculated using the root sum squared method:

$$B_r = \sqrt{\sum (b_i)^2} \tag{11}$$

For each measurement, the first step to determine the random uncertainty is to calculate the variance, Sx, of the sample data:

$$S_x = \sqrt{\frac{1}{n-1}\sum_{i=1}^{n}\left(x_i - \bar{X}\right)^2} \tag{12}$$

The mean variance, $S_{\bar{x}}$,is then estimated:

$$S_{\bar{x}} = \frac{S_x}{\sqrt{n}} \tag{13}$$

Then, the degrees of freedom, *df*, must be computed to get the 95% confidence interval *t*-statistic from statistics tables. This should combine all the degrees of freedom of both random and systematic uncertainties:

$$df = \frac{\left(\sum (S_{\bar{x},i})^2 + \sum \left(\frac{b_i}{2}\right)^2\right)^2}{\left(\sum \left((S_{\bar{x},i})^4 / df_i\right) + \sum \left(\frac{b_i}{2}\right)^4 / df_i\right)} \tag{14}$$

From this *df*, the corresponding t_{95} value can be found in statistics table. The experimental uncertainty, U_{ASME}, can then be determined for each data point based on the ASME method:

$$U_{ASME} = t_{95}\left[\left(\frac{B_r}{2}\right)^2 + (S_{\bar{x}})^2\right]^{0.5} \tag{15}$$

This number is presented as the error bars on the plot, as seen in Figure 9. Due to the highly precise measurement, the uncertainty is small, less than 0.5%, and does not show up well in Figure 9. Figure 12 shows a blown-up view of just one test run at a GVF of 21.4% to demonstrate the 95% confidence interval.

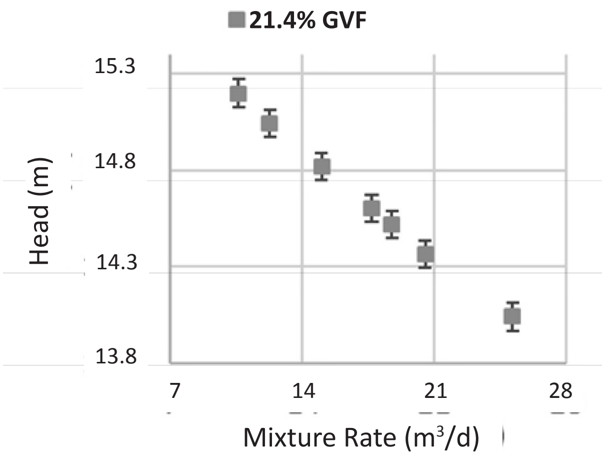

Figure 12: 95% confidence interval analysis.

CONCLUSIONS

This study experimentally investigated the effects of high viscosity oil and foamy oil flow on a single stage centrifugal pump performance. At the same time, the rheology between high viscosity single-phase oil and foamy oils was compared using the pipe viscometer. The correction factors had also been introduced to predict the performance of a centrifugal pump when handling foamy oils. Moreover, the following conclusions are drawn from the study:

• Up to a GVF of 37.8%, foamy oils had the same viscosity of dead oil and behaved as a Newtonian fluid.
• Up to GVF of 37.8%, foamy oils had similar pump increment pressure performance curves as single-phase oil with up to 8% difference in a comparable capacity. As a result, foamy oil induced a gain in pump head performance.
• Homogeneous model was unable to predict the pump pressure performance with acceptable accuracy.
• The new head and capacity correction factors for foamy flow were proposed. The prediction closely matched the experimental data, with an error less than 3% in both head and capacity.

ACKNOWLEDGEMENTS

The authors would like to acknowledge the support of the member companies of the Production and Drilling Research Project (PDRP) at New Mexico Institute of Mining and Technology.

NOMENCLATURE

ΔL	Differential Length (m)
ΔP	Differential Pressure (kPa)
cP	centipoise (cP)
D	Pipe Diameter (m)
ESP	Electrical Submersible Pump (N/A)
GOR	Gas-Oil-Ratio (N/A)
GVF	Gas Volume Fraction (N/A)
H	Head (m)
N	Rotational Speed (RPM)
Q	Volumetric Flow Rate (m^3/d)
Q_g	Gas Volumetric Flow Rate (mscf/d)
Q_l	Liquid Volumetric Flow Rate (m^3/d)
Q_m	Mixture Volumetric Flow Rate (m^3/d)
Q_o	Oil Volumetric Flow Rate (m^3/d)
R	Pipe Radius (m)
RPM	Rounds Per Minute (N/A)
U	Mean Velocity (m/s)
V	Volume (L)
VFD	Variable Frequency Drive (N/A)
Subscript	
g	Gas
l	Liquid
m	Mixture
o	Oil
Greek	
γ_w	Wall Shear Rate (Pa.s)
γn	Nominal Shear Rate (s^{-1})
λ_g	Gas Void Fraction (N/A)
ρ	Density (kg/m3)
ρm	Mixture Density (kg/m^3)
τw	Wall Shear Stress (Pa)

REFERENCES

1. Lea J. F. and Bearden J. L., “Effect of Gaseous Fluids on Submersible Pump Performance,” *Journal of Petroleum Technology*, **1982**, *34*, 2922-2930.
2. Pessoa R. and Prado M., “Experimental Investigation of Two-phase Flow Performance of Electrical Submersible Pump Stages,” in SPE Annual Technical Conference and Exhibition, New Orleans, **2000**.
3. Beltur R., Duran J., and Pessoa R., “Analysis of Experimental Data of ESP Performance under Two-phase Flow Conditions,” in SPE Production and Operations Symposium, Oklahoma City, **2003**.
4. Duran J. and Prado M., “ESP Stages Air-water Two-phase Performance: Modeling and Experimental Data,” Society of Petroleum Engineers, SPE-87627-MS, **2003**.
5. Fonseca Jr. R. d., Domingos P. V. S. R., and Reis D. C. d., “Experimental Evaluation of Behavior of Intermittent Flow in Scenario of Application of Electrical Submersible Pump,” in SPE Artificial Lift Conference, Salvador, Bahia, **2015**.
6. Trevisan F. E. and Prado M. G., “Experimental Investigation on the Viscous Effect on Two-phase Flow Patterns and Hydraulic Performance

of Electrical Submersible Pumps," in Canadian Unconventional Resources and International Petroleum Conference, Calgary, **2010**.
7. Maini B., "Foamy Oil Flow in Heavy Oil Production," *Journal of Canadian Petroleum Technology*, 06, *35*, **1996**.
8. Albartamani N. S., Ali S. M., and Lepski B., "Investigation of Foamy Oil Phenomena in Heavy Oil Reservoirs," in International Thermal Operations/Heavy Oil Symposium, Bakersfield, **1999**.
9. Alshmakhy A. B. and Maini B. B., "Foamy-oil Viscosity Measurement," *Journal of Canadian Petroleum Technology, 51,* **2012** .
10. Solano E. A., "Viscous Effects on the Performance of Electro Submersible Pump (ESP's)," The University of Tulsa, Tulsa, **2009**.
11. J. Gamboa and M. Prado, "Experimental Study of Two-phase Performance of an Electric-Submersible-Pump Stage," SPE Production & Operations, **2012**.
12. Sun D. and Prado M., "Single-phase Model of ESP's Head Performance," in SPE Production and Operations Symposium, Oklahoma City, **2003**.
13. Aadnoy B. S., Cooper I., Miska S. Z., Mitchell R. F. et al., "Advanced Wellbore Hydraulics," in Advanced Drilling and Well Technology, Richardson, TX, Society of Petroleum Engineers, **2009**, 197-198.